Efficient Quasi-TEM Frequency-Dependent Analysis of Lossy Multiconductor Lines Through a Fast Reduced-Order FEM Model

Francesco Bertazzi, Giovanni Ghione, *Senior Member, IEEE*, and Michele Goano, *Member, IEEE*

***Abstract*—An efficient finite-element reduced-order quasi-TEM model for the frequency-dependent characteristics of lossy multiconductor transmission lines is presented. Conductor losses are evaluated as functions of frequency through a magneto-quasi-static model. Numerically generated problem-matched basis functions reduce the problem size and, therefore, the CPU time required by frequency sweeps without appreciable loss of accuracy. The proposed approach is applied to complex coplanar waveguides and to multiconductor interconnects; its results are compared with quasi-analytical techniques and with the full-wave finite-element method.**

***Index Terms*—Coplanar waveguides (CPWs), Damascene multilevel interconnects, electrooptic modulators, finite-element method (FEM), magneto-quasi-static problem, micromachined CPWs, model order reduction, multiconductor transmission lines (MTLs), ohmic losses, skin effect.**

I. Introduction

In MANY analog, digital, and opto-electronic high-speed circuit applications, accurate, but computationally efficient, models are required for simple or multiconductor transmission lines (MTLs), often allowing for complex geometries and materials. These may include arbitrary cross sections, anisotropic and lossy substrates, and metallic regions of finite conductivity whose thickness may be smaller or larger than the skin penetration depth within the frequency range of interest. Moreover, the design of high-speed digital circuits involves the accurate prediction of reflection, distortion, and crosstalk in interconnects, thus stressing the importance of efficient and accurate techniques for the wide-band modeling of lossy multiconductor lines.

Among the quasi-static or full-wave (FW) analysis techniques allowing for anisotropic materials, conductor and dielectric losses, and arbitrary (e.g., nonplanar) geometries, the finite-element method (FEM) is probably the most flexible and powerful. Different FW-FEM formulations of the waveguide problem have been presented in the literature [1]; recently, a general three-component formulation of the lossy anisotropic waveguide problem has been introduced [2]. The FW approach leads to a large (albeit sparse) generalized eigenvalue problem, whose solutions are the complex modal propagation constants [3]–[5]. Although acceleration methods are available to improve the computational efficiency of the FW model (see, e.g., the reduced-order technique proposed in [3]), this approach is still computationally too intensive for the direct inclusion in computer-aided design (CAD) tools for circuit analysis and design, above all in the multiconductor case. On the other hand, in many applications (e.g., high-speed digital or analog integrated circuits), the size reduction of the line cross section makes modal dispersion virtually negligible for quasi-TEM propagation on a wide frequency range; in such cases, the quasi-static FEM model is a viable alternative to the FW analysis.

This paper introduces a quasi-static FEM technique for the efficient evaluation of the frequency-dependent characteristic parameters of lossy multiconductor transmission lines (MTLs); the method proposed is a generalization of the approach presented in [6] by Bertazzi *et al.* The extraction of the per-unit-length (p.u.l.) inductance and resistance matrices of MTLs is based on the solution of the two-dimensional (2-D) magneto-quasi-static problem for the magnetic potential. The formulation of the magneto-quasi-static problem leads, in contrast with the integrodifferential formulation introduced in [7], to a sparse matrix equation.

In many practical cases the frequency dispersion of the quasi-TEM MTL p.u.l. parameters, related to material losses, cannot be neglected. The accurate analysis of the MTL response in the presence of wide-band signals thus requires the computation of the MTL p.u.l. parameters (in particular, the series impedance matrix) versus frequency. Despite the improved efficiency of the quasi-TEM with respect to the FW approach, repeating the quasi-TEM analysis for many frequency points in the range of interest still leads to a computationally intensive problem. Reduced-order approaches previously applied to the efficient wide-band solution of the FW problem [3] can be readily extended to the computation of frequency-dependent quasi-TEM parameters. Such approaches are based on the numerical generation of an orthonormalized set of problem-matched basis functions [8]. In this paper, a robust fast frequency-sweep technique, based on the concept of problem-matched basis functions, is proposed for the solution of the eddy–current problem in a lossy MTL. This technique allows for a drastic reduction of the number of basis functions, while still accurately approximating the original response over a broad frequency range.

This paper is organized as follows. In Section II, the quasi-TEM formulation is reported. Section III presents the

Manuscript received January 13, 2003; revised April 21, 2003. This work was supported in part by Pirelli Laboratories and by the Centro di Eccellenza per le Comunicazioni Multimediali under Project WP2.1 and Project WP2.3.

The authors are with the Dipartimento di Elettronica, Politecnico di Torino, I-10129 Turin, Italy (e-mail: ghione@polito.it).

Digital Object Identifier 10.1109/TMTT.2003.815875

numerical procedure for the generation of problem-specific basis functions. The extraction process for the quasi-TEM circuit parameters of the MTL is described in Section II-C. Several examples are discussed in Section IV, where excellent agreement is demonstrated with the FW-FEM. Some concluding remarks are finally reported in Section V.

II. Quasi-TEM Model

Consider an MTL consisting of K conductors (including the reference conductor), embedded in a lossy nonhomogeneous dielectric medium, characterized by diagonal permittivity and permeability tensors $\tilde{\epsilon}, \mu$. Dielectric losses are included in the imaginary part of the permittivity tensor. Let us assume that the line is uniform along the z-axis, and let the electrodes have arbitrary cross sections Ω_k and finite conductivity σ_k, which we assume as constant on the kth conductor cross section.

Assuming quasi-TEM modal propagation, the electric and magnetic problems can be decoupled, thus leading to the separate evaluation of the transverse magnetic and electric fields, respectively. The transverse H-field is evaluated through an eddy–current formulation, which assumes that the transverse electric field in the conductors is negligible, whereas in the same regions, a small z-component of the electric field exists, related to the conduction current density J_z. The transverse E-field outside the conductors is computed through a conventional quasi-static approach based on the solution of the Laplace equation for the electric potential. The two formulations immediately lead to the definition of the p.u.l. series impedance and parallel admittance, respectively, of the MTL.

A. Transverse H-Field (Eddy–Current) Formulation

In the present approach, a vector potential $\vec{A}$ and a scalar potential ϕ are chosen as unknown variables. They are defined through the electric and magnetic fields as

$$\begin{cases} \vec{B} = \nabla \times \vec{A} \\ \vec{E} = -\nabla_t \phi - \left(\dfrac{\partial \phi}{\partial z}\right) \hat{z} - j\omega \vec{A}. \end{cases}$$

From potential theory, it is well known that the vector potential $\vec{A}$ is not unique unless a gauge condition is imposed. Using the Lorentz condition, an inhomogeneous Helmholtz equation for the magnetic potential $\vec{A}$ results [9] as follows:

$$-\nabla^2 \vec{A} - \omega^2 \mu \tilde{\epsilon} \vec{A} = \mu \vec{J}^{(s)} \tag{1}$$

where $\vec{J}^{(s)}$ is the impressed current density. If quasi-TEM propagation is assumed, $\vec{J}^{(s)}$ has only one component along the z-direction, which is given by the product of the metal conductivity times the longitudinal impressed electric field $\mathcal{E}$; since the transverse electric-field components are taken to be negligible inside the electrodes, the impressed electric field $\mathcal{E} = -\partial\phi/\partial z$ may be taken constant over the metal conductors [10]

$$\vec{J}^{(s)}(x,y) = \sigma_k \mathcal{E}_k \hat{z} \qquad \forall (x,y) \in \Omega_k. \tag{2}$$

Substituting (2) into (1) and neglecting displacement currents, (1) simplifies to

$$-\nabla_t^2 A_z + j\omega\mu\sigma_k A_z = \mu\sigma_k \mathcal{E}_k \qquad \forall (x,y) \in \Omega_k \tag{3a}$$

$$\nabla_t^2 A_z = 0 \qquad \forall (x,y) \in \Omega_d \tag{3b}$$

where Ω_d denotes the dielectric region outside the metal conductors. After the computational domain Ω has been divided into a set of triangular elements, the application of Galerkin's procedure to (3) yields the following matrix equation:

$$(\boldsymbol{R} + j\omega\mu \boldsymbol{T})\boldsymbol{A} = \mu \boldsymbol{J} \tag{4}$$

where $\boldsymbol{J} = \sum_{k=1}^{K} \sigma_k \mathcal{E}_k \boldsymbol{N}_k$ and

$$\boldsymbol{R} = \sum_{e \in \Omega} \sigma_e \iint_e \left(\{N_x\}\{N_x\}^T + \{N_y\}\{N_y\}^T \right) dxdy \tag{5a}$$

$$\boldsymbol{T} = \sum_{e \in \Omega} \iint_e \{N\}\{N\}^T dxdy \tag{5b}$$

$$\boldsymbol{N}_k = \sum_{e \in \Omega_k} \iint_e \{N\} dxdy. \tag{5c}$$

Explicit forms of the column shape function vectors $\{N\}$, $\{N_x\}$, and $\{N_y\}$, and analytical expressions of the integrals in (5) are given in [11]. Homogeneous Dirichlet and Neumann boundary conditions are assumed on the subsets Γ_D and Γ_N, respectively, of the whole boundary Γ of the domain $\Omega(\Gamma = \Gamma_D \cup \Gamma_N)$

$$A_z = 0, \qquad \text{on } \Gamma_D \tag{6a}$$

$$\nabla_t A_z \cdot \hat{n} = 0, \qquad \text{on } \Gamma_N \tag{6b}$$

where Γ_D and Γ_N are electric and magnetic walls, respectively, and $\hat{n}$ is the outward normal vector. Of course, in assembling (4), the (natural) boundary conditions (6b) do not need to be explicitly enforced. Once (3) has been solved for a given impressed current density, the MTL currents may be evaluated integrating the total current density $J_z(x,y) = J_z^{(s)}(x,y) - j\omega\sigma A_z(x,y)$ over the electrodes

$$I_k = S_k \sigma_k \mathcal{E}_k - j\omega\sigma_k \boldsymbol{N}_k^T \boldsymbol{A} \tag{7}$$

where S_k is the conductor cross area. In order to compute the p.u.l. series impedance matrix of the MTL, we compute K linearly independent solutions of (3), obtained by setting a unit impressed electric field $\mathcal{E}$ in each of the conductors in succession. The $K \times K$ p.u.l. impedance matrix $[\mathcal{Z}] = [\mathcal{R}] + j\omega[\mathcal{L}]$ can then be readily evaluated from the generalized telegraphers' equation

$$[\mathcal{Z}] = [\mathcal{E}][I]^{-1}$$

where $[\mathcal{E}]$ is the $K \times K$ identity matrix whose columns represent the electric-field excitations of the MTL, and the columns of $[I]$ are the corresponding currents computed according to (7).

Notice that the present formulation, when compared to the conventional integrodifferential equation introduced for the two-dimensional eddy–current problem in [7] and [12], leads to the finite-element matrix equation (4) which can be efficiently handled by a sparse linear solver. Also, (4) may be efficiently

solved for any current excitation once a sparse factorization of the coefficient matrix has been obtained.

B. Transverse E-Field Formulation

To evaluate the parallel p.u.l. admittance matrix, the electrostatic potential ϕ is computed from Laplace's equation

$$\nabla_t \cdot (\tilde{\epsilon} \nabla_t \phi) = 0$$

subject to the boundary conditions that the potential ϕ be constant over each conductor Ω_k. Application of the Galerkin procedure leads to the sparse problem

$$\boldsymbol{K}\phi = \boldsymbol{q}$$

where $\boldsymbol{q}$ originates from the applied voltages on the metal conductors and $\boldsymbol{K}$ is a sparse matrix whose expression can be found in [5]. The p.u.l. admittance matrix $[\mathcal{Y}] = [\mathcal{G}] + j\omega[\mathcal{C}]$ can be conveniently evaluated from the complex electrostatic energy matrix obtained applying unit voltage on each conductor in succession as follows:

$$[V]^{\dagger}[\mathcal{Y}][V] = j\omega(\phi_1, \ldots, \phi_K)^{\dagger}\boldsymbol{K}(\phi_1, \ldots, \phi_K)$$

where $\dagger$ is the conjugate transpose operator, $[V]$ is a $K \times K$ identity matrix whose columns correspond to the voltage excitations of the active strips, and the column vectors $\phi_1, \ldots, \phi_K$ are the finite-element representations of the induced electrostatic potentials. Notice that, if dielectric losses are characterized by a frequency-independent loss tangent, the conductance matrix $[\mathcal{G}]$ is a linear function of frequency.

C. Modal Analysis

As well known, a system of K active conductors supports K quasi-TEM propagation modes, whose phase velocities and characteristic impedances can be derived through standard techniques from multiconductor analysis. Once the p.u.l. matrices $[\mathcal{R}(\omega)]$, $[\mathcal{L}(\omega)]$, $[\mathcal{C}(\omega)]$, and $[\mathcal{G}(\omega)]$ have been computed for each frequency, the modal propagation constants γ_k can be derived as the square roots of the eigenvalues of the matrix product $[\mathcal{Y}][\mathcal{Z}]$

$$[\mathcal{Y}][\mathcal{Z}] = [M][\Gamma]^2[M]^{-1}$$

where the columns of matrix $[M]$ are the modal currents in the active electrodes, and $[\Gamma] = \mathrm{diag}\{\gamma_1, \ldots, \gamma_K\}$. The diagonal modal characteristic impedance matrix may be computed according to the power–current definition as [13]

$$[Z] = [\Gamma]^{-1}[M]^T[\mathcal{L}][M]^*.$$

III. Reduced-Order Model

Although modal dispersion is negligible for quasi-TEM lines, losses are responsible for strong dispersion from the low-frequency *RC* range to the skin-effect *LC* regime and the very p.u.l. parameters (in particular, the resistance and inductance matrices) are, in principle, frequency dependent. In this study, conductor ohmic loss is assumed to be the dominant loss mechanism, and dielectric losses are modeled by a frequency-independent loss tangent. Consequently, the electrostatic potential ϕ does not depend on frequency, whereas the magneto-quasi-static analysis should be repeated for many frequency sampling points in the range of interest. A fast frequency-sweep technique for the solution of the skin-effect problem is presented here. Notice, however, that this technique may also be applied to the electrostatic problem if dielectric losses are represented through a constant conductivity or other physics-based models [14].

Several order-reduction techniques have been presented during the last few years for the solution of electromagnetic problems (see, e.g., [3] for a review). Recently, the concept of problem-matched basis functions has received much interest; such basis functions are extremely efficient in the (wide-band) representation of the unknown, thus drastically reducing the CPU time. In [8], a novel technique for the numerical generation of an orthonormalized set of problem-matched basis functions has been introduced with application to the scattering problem. The technique in [8] (see [3] for an application to the FW modal analysis) is applied to the solution of the quasi-static problem as follows. The magnetic potential A is evaluated with full accuracy via the approach described in Section II at P frequency points $\omega = \omega_1, \ldots, \omega_P$ chosen in the band of interest. Fast frequency sweeps are made possible through the generation of problem-specific basis functions derived from this exact analysis at the P sampling points. In order to define an orthonormalized set of problem-matched basis functions, the FEM solution vectors $\boldsymbol{A}(\omega_p)$ are arranged column-wise in a $N \times P$ matrix $\boldsymbol{X}$, which is then subjected to the reduced singular value decomposition (SVD) [15]

$$\boldsymbol{X} = \boldsymbol{U}\Sigma\boldsymbol{V}^{\dagger}$$

where $\boldsymbol{U}$ is an $N \times P$ matrix whose columns are the singular vectors, $\boldsymbol{\Sigma}$ is a $P \times P$ diagonal matrix with positive elements (singular values), and $\boldsymbol{V}$ is a $P \times P$ unitary matrix. The significance of each singular vector in the representation of the unknown is measured by the corresponding singular value. Since they range over several orders of magnitude, not all of the singular vectors are needed to get accurate results [3]. Let $Q \leq P$ then be the number of singular vectors assumed to be adequate to represent the unknown. The selected singular vectors define a set of problem-matched basis functions of a low-dimensional subspace Ξ that contains the potential representation, at least in the band of interest. System (4) may be written in compact form as $(\boldsymbol{M}_0 + \omega\boldsymbol{M}_1)\boldsymbol{A} = \boldsymbol{b}$, where $\boldsymbol{M}_\alpha$, $\alpha = 0, 1$ are frequency-independent matrices, which can be derived by inspection of (4). The restriction of large-scale equation (4) in the subspace Ξ yields the reduced-order model

$$\left(\boldsymbol{U}_Q^{\dagger}\boldsymbol{M}_0\boldsymbol{U}_Q + \omega\boldsymbol{U}_Q^{\dagger}\boldsymbol{M}_1\boldsymbol{U}_Q\right)\tilde{\boldsymbol{A}} = \boldsymbol{U}_Q^{\dagger}\boldsymbol{b} \tag{8}$$

where $\tilde{\boldsymbol{A}}$ is the unknown in the reduced-order representation and matrix $\boldsymbol{U}_Q$ consists of the first Q singular vectors selected. Notice that the MTL currents may be directly computed in the reduced-order representation as

$$I_k = S_k\sigma_k\mathcal{E}_k - j\omega\sigma_k\left(\boldsymbol{N}_k^T\boldsymbol{U}_Q\right)\tilde{\boldsymbol{A}} \tag{9}$$

Equation (8) has size $Q \times Q$, and may be easily solved by a direct method for each frequency value. Moreover, by inspection of the dynamic range of the singular values, the accuracy level of the procedure can be controlled: if the P singular values have a small dynamic range, not enough information is available, and

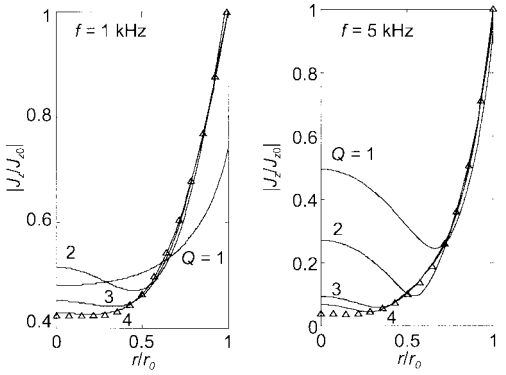

Fig. 1. Comparison between the normalized magnitude of the current density $|J_z/J_{z0}|$ in the cylindrical wire at $f = 1$ kHz and $f = 5$ kHz as a function of the radius of the wire r/r_o evaluated analytically (triangles) and with the present numerical approach for $Q = 1, 2, 3, 4$ (solid lines).

the frequency sampling rate should be increased. In all the numerical examples considered in this study, the P sampling frequencies have been distributed with a uniform spacing over the frequency range of interest. The very good accuracy achieved by this simple approach with a small number of samples probably makes irrelevant the refinement of the sampling frequency selection strategy.

As an example of the properties of the reduced-order algorithm in a case where the exact analytical solution is available, a copper cylindrical conductor (radius $r = 5$ mm, conductivity $\sigma = 5.8 \times 10^7$ S/m) has been considered. The magneto-quasi-static problem has been solved via the standard approach at $P = 10$ frequency points chosen in the range from 0.1 to 1000 kHz; the reduced-order model was then obtained. Fig. 1 compares the magnitude of the total current density evaluated at two frequencies with its exact analytical expression [9] and through the present reduced-order model with $Q = 1, 2, 3, 4$ problem-matched basis functions. The range of the singular values is approximately eight orders of magnitude. Notice the remarkable accuracy that may be achieved in the modeling of the frequency-dependent current density by using only the first four basis functions, whose corresponding (normalized) singular values are 1, 0.0159, 0.0018, and 0.0004. As a rule-of-thumb, basis functions corresponding to singular values at least three orders of magnitude below the dominant one can be safely neglected.

IV. Results

In order to show the effectiveness of the proposed numerical technique, three different structures have been considered: a ridge-type coplanar waveguide (CPW) on a lithium–niobate substrate, a set of micromachined CPWs, and a typical interconnect structure. Excellent agreement is demonstrated (in the frequency range where modal dispersion is negligible) with the FW solution, at less than one-tenth of its computational cost.

A. Ridge Modulator

The design and optimization of electrooptic modulators on $LiNbO_3$ substrates demand precise modeling of their microwave propagation characteristics because of the conflicting requirements in terms of velocity matching, low

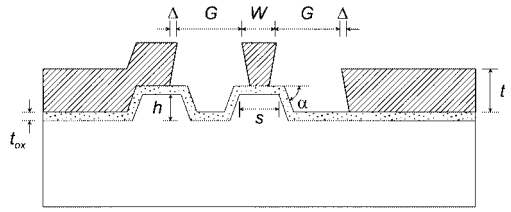

Fig. 2. Cross section of a ridge-type CPW. The geometrical parameters are $t = 29\,\mu$m, $W = 8\,\mu$m, $G = 25\,\mu$m, $t_{ox} = 0.6\,\mu$m, $h = 3.5\,\mu$m, $s = 9\,\mu$m, $\alpha = 70°$, and $\Delta = 1\,\mu$m.

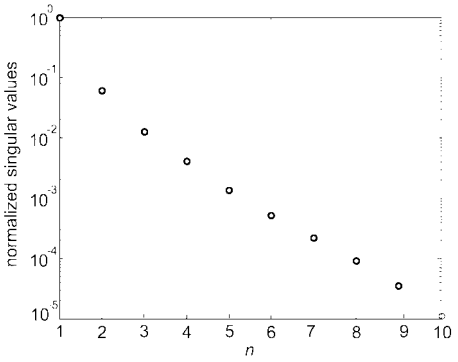

Fig. 3. Normalized singular values (up to order 10) of the reduced-order model for the ridge-type CPW shown in Fig. 2.

microwave attenuation, and superposition between the optical and microwave fields [16]. In the ridge-type modulator (see Fig. 2) introduced in [17] and [18], synchronous coupling with the optical signal is achieved by removing the high dielectric-constant lithium niobate (the relative permittivity constants of the Z-cut X-propagating $LiNbO_3$ substrate are 28 and 43 perpendicular and parallel to the substrate surface, respectively, and the loss tangent is $\tan\delta_s = 0.004$) around the center conductor, and inserting a low dielectric constant SiO_2 buffer layer ($\epsilon_r = 3.90$, $\tan\delta_b = 0.016$) underneath the gold electrodes ($\sigma = 4.1 \times 10^7$ S/m). The CPW structure under investigation is shown in Fig. 2, and has been already studied in [5]. The realistic metallization undercutting is a typical result of galvanic processes. The magneto-static problem has been solved at $P = 10$ frequency points. The range of the singular values is approximately five orders of magnitude (see Fig. 3), which confirms that the frequency sampling rate is sufficient to represent the solution. The microwave effective index $n_{\rm eff}$, the attenuation constant α (in decibels per centimeter), and the characteristic impedance $Z(\Omega)$ have been computed versus frequency with $Q = 2, 3, 5$ problem-matched basis functions (see Fig. 4). The frequency variations of the circuit parameters of the line are correctly modeled with $Q = 5$ problem-matched basis functions over a bandwidth of 100 GHz. Notice that the current density distribution inside lossy conductors drastically changes within the selected frequency range. An excellent agreement may be observed between the present quasi-static analysis and the FW-FEM solution [3]. The microwave effective index and characteristic impedance in [5] are also in excellent agreement with this study and are not reported for clarity. In this approach, the microwave attenuation α includes the contribution of dielectric losses and, therefore, is significantly higher at high frequencies [14] than the familiar $\sqrt{f}$ behavior presented in [5]. The small discrepancies, arising at higher frequencies between

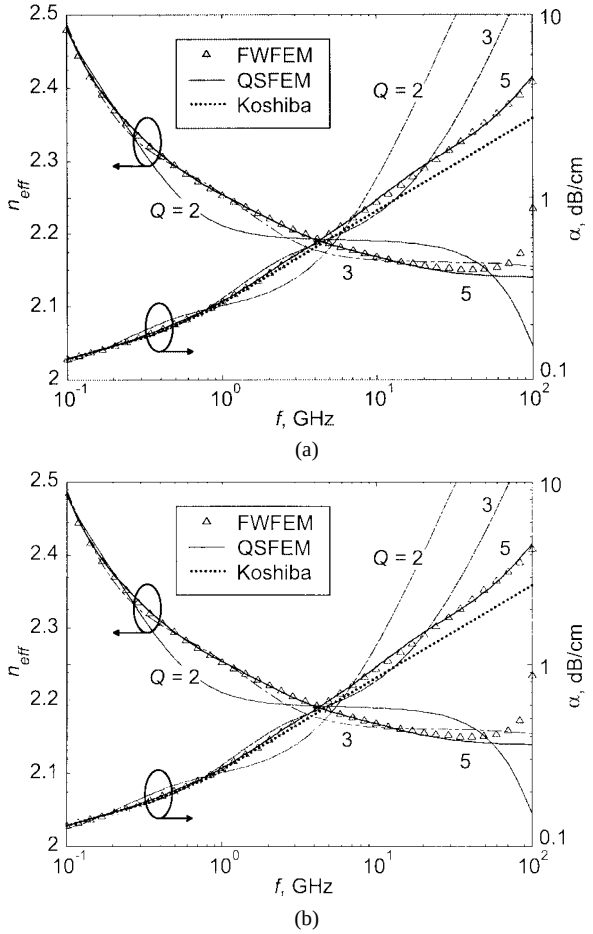

Fig. 4. (a) Microwave effective index $n_{\rm eff}$, attenuation α (in decibels per centimeter), and (b) complex characteristic impedance $Z_c(\Omega)$ of the ridge-type CPW shown in Fig. 2, computed with the FW-FEM (triangles) and present magnetic-quasi-static model with $Q = 2, 3, 5$ problem-matched basis functions. Characteristic impedances have been computed according to the power–current definition.

quasi-TEM model and FW solutions, are related to the onset of higher order substrate modes [19]. Owing to the very small transverse line dimension, modal dispersion in this structure is virtually negligible over the whole frequency range.

The CPU time required by a MATLAB[1] implementation of the proposed quasi-static FEM on a personal computer equipped with an 800-MHz Intel Pentium III processor is 0.6 s for the solution of the electric problem, 1.4 s for the solution of the magnetic problem at each frequency point, and 0.4 s for the SVD and the reduced-order frequency sweep. On the same mesh, FW-FEM analysis using zeroth-order curl-conforming elements takes 30 s at each frequency point.

B. Micromachined CPWs

Conventional CPWs exhibit high conductor losses at high and low characteristic impedance due to narrowing of the center conductor and slot width, respectively. Recently, a novel class of CPW structures, in which the electrodes are elevated with micromachining techniques, has been introduced to achieve low losses over a broad impedance range [20], [21]. In the present example, three structures are considered (see Fig. 5), i.e., the

[1]MATLAB is a registered trademark of The MathWorks Inc., Natick, MA.

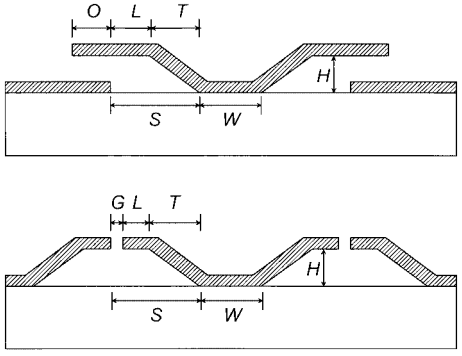

Fig. 5. Cross section of micromachined OCPW and ECPW.

elevated coplanar waveguide (ECPW) (the center electrode and ground planes are elevated to the same height H), the overlay coplanar waveguide (OCPW) (the edges of the center conductor are elevated and partially overlapped with the ground), and the conventional CPW. The ground-to-ground spacing $(W + 2S)$ was fixed at 170 μm for this comparison. The center conductor width W was changed to vary the characteristic impedance of the conventional CPW. The gap G of the ECPW was changed from 3 to 27 μm; the overlap O of the OCPW was changed from 50 to -30 μm (negative values represent separation). All the conductor layers have been assumed to be 3-μm-thick electroplated gold on a glass substrate with nonnegligible dielectric losses ($\epsilon_r = 4.6$, $\tan\delta = 0.02$). In Fig. 6(a), the *in vacuo* microwave attenuation constant α_0 of the OCPW and ECPW at $f = 50$ GHz is plotted versus the characteristic impedance Z_0. The quasi-static technique is in excellent agreement with the reference results obtained with the numerical conformal mapping (CM) technique proposed in [22] (numerical CM represents an ideal reference tool for *in vacuo* CPWs of arbitrary cross section since Z_0 is evaluated exactly and α_0 is extremely well described in the microwave range). The same agreement may be observed in Fig. 6(b) between the present approach and the FW-FEM analysis when a dielectric substrate is included in the simulation. The computation time of quasi-static analysis is approximately one-tenth of FW analysis. As expected, compared with the conventional CPW, the OCPW shows lower losses over a broad impedance range. In the OCPW design, current crowding at the edges of the conductors is avoided by controlling the characteristic impedance with the overlap parameter O, and a screening effect from substrate losses is achieved by concentrating the electric field in the parallel-plate region between the center electrode and ground electrodes [21].

C. Damascene Multiconductor Interconnect Structure

The analysis and design of high-speed multiconductor interconnects has become, during the last few years, increasingly important in microelectronics (see, e.g., [23]). As an example of application, a Damascene Cu multiconductor interconnect bus (shown in Fig. 7) has been considered. The permittivity of the embedding dielectric (SiO_2) is $\epsilon_r = 3.9$ with loss tangent $\tan\delta = 0.016$. All the signal lines and reference conductors are made of copper, with conductivity $\sigma = 5.8\times10^7$ S/m. Eight frequency sampling points have been evenly spaced in the interval between 1–40 GHz. The range of the singular values was found

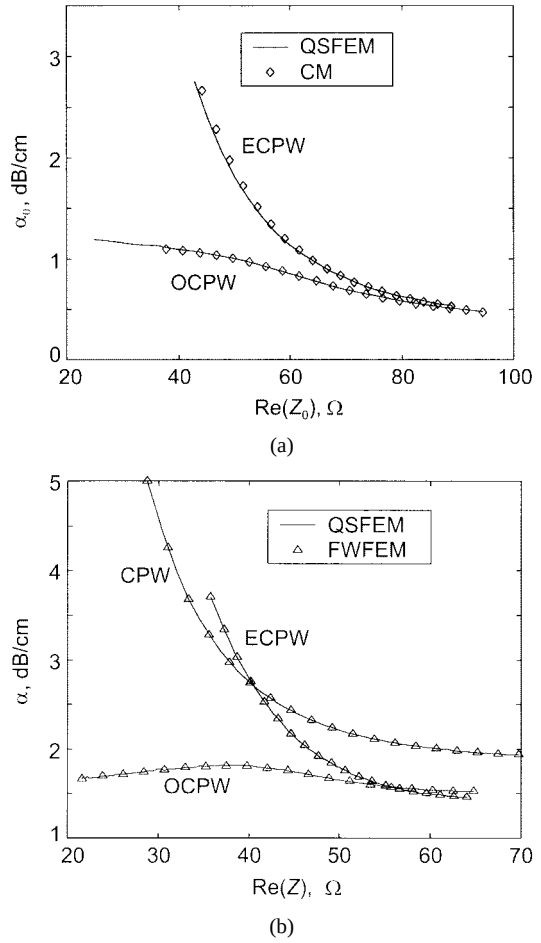

Fig. 6. (a) *In vacuo* microwave attenuation α_0 (in decibels per centimeter) versus characteristic impedance $Z_0(\Omega)$ of the OCPW and ECPW (the gold electrode conductivity is $\sigma = 4.1 \times 10^7$ S/m), computed with numerical CM (diamonds) and the present magneto-quasi-static model (solid lines) at $f = 50$ GHz. (b) Microwave attenuation α (in decibels per centimeter) versus characteristic impedance $Z(\Omega)$ of the OCPW, ECPW, and CPW on a 520-μm-thick glass substrate ($\epsilon_r = 4.6$, $\tan\delta = 0.02$) computed with the FW-FEM (triangles) and the present magneto-quasi-static model (solid lines), at $f = 50$ GHz. The geometrical parameters are $t = 3\ \mu$m, $W = 28\ \mu$m, $S = 71\ \mu$m, $O = 10\ \mu$m, $H = 15\ \mu$m, and $T = 40\ \mu$m.

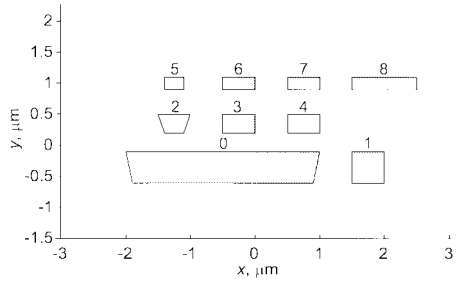

Fig. 7 Cross section of an eight-conductor Cu Damascene interconnect; conductor 0 is the return (reference) line. The embedding dielectric is SiO_2.

to be over ten orders of magnitude. By discarding the singular values three orders of magnitude below the dominant one, we only selected the first $Q = 11$ singular values. Fig. 8 shows the microwave effective index $n_{\rm eff}$ and attenuation α of the quasi-TEM modes of the multiconductor system computed with the present approach and FW-FEM analysis. Excellent agreement may be observed between quasi-static analysis and FW

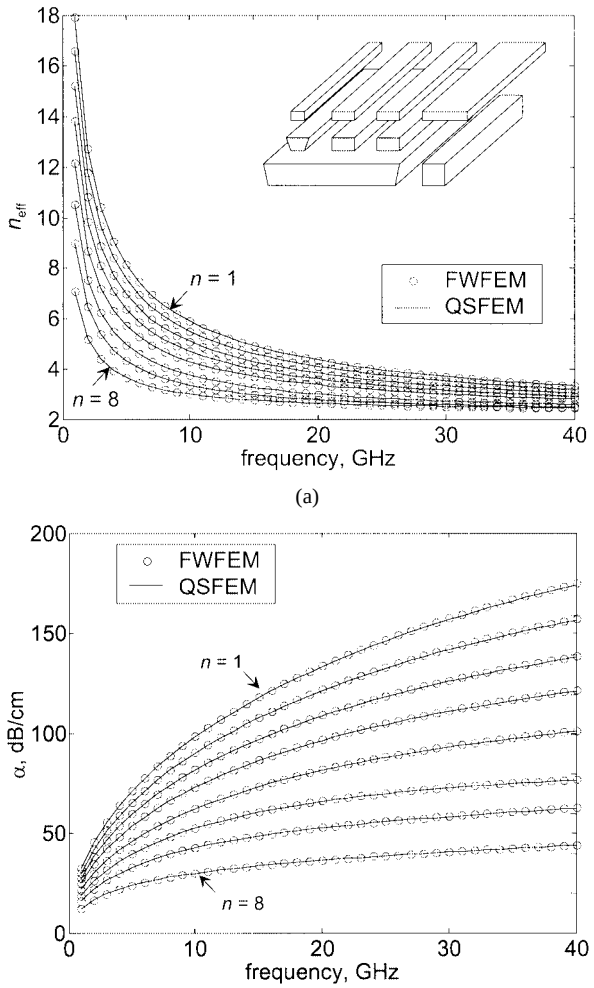

Fig. 8 (a) Microwave effective index $n_{\rm eff}$ and (b) attenuation constant α (in decibels per centimeter) of the quasi-TEM modes of the interconnect structure shown in Fig. 7 computed with FW-FEM (circles) and the present model (solid lines). The eight quasi-TEM modes are ordered according to decreasing $n_{\rm eff}$ and α.

results up to 40 GHz and beyond. Owing to the submicrometer cross section of the interconnect, low-frequency RC dispersion effects are noticeable up to more than 10 GHz. Moreover, although the dielectric is homogeneous, the modal effective permittivities are quite different from each other and larger than the SiO_2 permittivity even at the highest frequency considered. This slow-wave effect can be attributed to the magnetic-field penetration into the conductors, which is significant even at 40 GHz, where the skin-effect penetration depth is $\delta = 0.33\ \mu$m, i.e., comparable with the conductor thickness. Thus, it can be concluded that, due to the effect of losses, a purely TEM model is altogether inadequate to simulate the propagation characteristics of this kind of interconnect structures.

V. Conclusion

An FEM-based fast and accurate reduced-order model has been developed for the computation of the frequency-dependent characteristic p.u.l. parameters of multiconductor lines. Several examples have been presented concerning high-speed structures for analog and digital applications. Excellent agreement with

FW methods has been achieved at a fraction of their computational cost.

REFERENCES

[1] B. M. Dillon and J. P. Webb, "A comparison of formulations for the vector finite element analysis of waveguides," *IEEE Trans. Microwave Theory Tech.*, vol. 42, pp. 308–316, Feb. 1994.

[2] P. Savi, I.-L. Gheorma, and R. D. Graglia, "Full-wave high-order FEM model for lossy anisotropic waveguides," *IEEE Trans. Microwave Theory Tech.*, vol. 50, pp. 495–500, Feb. 2002.

[3] F. Bertazzi, O. A. Peverini, M. Goano, G. Ghione, R. Orta, and R. Tascone, "A fast reduced-order model for the full-wave FEM analysis of lossy inhomogeneous anisotropic waveguides," *IEEE Trans. Microwave Theory Tech.*, vol. 50, pp. 2108–2114, Sept. 2002.

[4] S. V. Polstyanko, R. Dyczij-Edlinger, and J.-F. Lee, "Fast frequency sweep technique for the efficient analysis of dielectric waveguides," *IEEE Trans. Microwave Theory Tech.*, vol. 45, pp. 1118–1126, July 1997.

[5] M. Koshiba, Y. Tsuji, and M. Nishio, "Finite-element modeling of broad-band traveling-wave optical modulators," *IEEE Trans. Microwave Theory Tech.*, vol. 47, pp. 1627–1633, Sept. 1999.

[6] F. Bertazzi, F. Carbonera, M. Goano, and G. Ghione, "FEM-based reduced-order model for steady-state skin-effect analysis in lossy lines," in *IEEE MTT-S Int. Microwave Symp. Dig.*, Seattle, WA, June 2002, pp. 2025–2028.

[7] A. Konrad, "Integrodifferential finite element formulation of two-dimensional steady-state skin effect problems," *IEEE Trans. Magn.*, vol. MAG-18, pp. 284–292, Jan. 1982.

[8] C. K. Aanandan, P. Debernardi, R. Orta, R. Tascone, and D. Trinchero, "Problem-matched basis functions for moment method analysis—an application to reflection gratings," *IEEE Trans. Antennas Propagat.*, vol. 48, pp. 35–40, Jan. 2000.

[9] S. Ramo, J. R. Whinnery, and T. Van Duzer, *Fields and Waves in Communication Electronics*, 3rd ed. New York: Wiley, 1994.

[10] J. Aguilera, R. Marqués, and M. Horno, "Quasi-TEM surface impedance approaches for the analysis of MIC and MMIC transmission lines, including both conductor and substrate losses," *IEEE Trans. Microwave Theory Tech.*, vol. 43, pp. 1553–1558, July 1995.

[11] M. Koshiba, S. Maruyama, and K. Hirayama, "A vector finite element method with the high-order mixed-interpolation-type triangular elements for optical waveguiding problems," *J. Lightwave Technol.*, vol. 12, pp. 495–502, Mar. 1994.

[12] G. I. Costache, "Finite element method applied to skin-effect problems in strip transmission lines," *IEEE Trans. Microwave Theory Tech.*, vol. MTT-35, pp. 1009–1013, Nov. 1987.

[13] G. G. Gentili and M. Salazar-Palma, "The definition and computation of modal characteristic impedance in quasi-TEM coupled transmission lines," *IEEE Trans. Microwave Theory Tech.*, vol. 43, pp. 338–343, Feb. 1995.

[14] K. M. Coperich, J. Morsey, A. C. Cangellaris, and A. Ruehli, "Physically consistent transmission line models for high-speed interconnects in lossy dielectrics," in *IEEE Electrical Performance of Electronic Packaging Topical Meeting*, Cambridge, MA, Oct. 2001, pp. 247–250.

[15] G. H. Golub and C. F. Van Loan, *Matrix Computations*, 3rd ed. Baltimore, MD: The John Hopkins Univ. Press, 1996.

[16] N. Dagli, "Wide-bandwidth lasers and modulators for RF photonics," *IEEE Trans. Microwave Theory Tech.*, vol. 47, pp. 1151–1171, July 1999.

[17] K. Noguchi, H. Miyazawa, and O. Mitomi, "Frequency-dependent propagation characteristics of coplanar waveguide electrode on 100 GHz Ti : $LiNbO_3$ optical modulator," *Electron. Lett.*, vol. 34, no. 7, pp. 661–663, Apr. 1998.

[18] K. Noguchi, O. Mitomi, and H. Miyazawa, "Millimeter-wave Ti : $LiNbO_3$ optical modulators," *J. Lightwave Technol.*, vol. 16, pp. 615–619, Apr. 1998.

[19] A. A. Oliner, "Types and basic properties of leaky modes in microwave and millimeter-wave integrated circuits," *IEICE Trans. Electron.*, vol. E83-C, no. 5, pp. 675–686, May 2000.

[20] H.-T. Kim, S. Jung, J.-H. Park, C.-W. Baek, Y.-K. Kim, and Y. Kwon, "A new micromachined overlay CPW structure with low attenuation over wide impedance ranges and its application to low-pass filters," *IEEE Trans. Microwave Theory Tech.*, vol. 49, pp. 1634–1639, Sept. 2001.

[21] ——, "A new micromachined overlay CPW structure with low attenuation over wide impedance ranges," in *IEEE MTT-S Int. Microwave Symp. Dig.*, vol. 1, Boston, MA, June 2000, pp. 299–302.

[22] M. Goano, F. Bertazzi, P. Caravelli, G. Ghione, and T. A. Driscoll, "A general conformal-mapping approach to the optimum electrode design of coplanar waveguides with arbitrary cross section," *IEEE Trans. Microwave Theory Tech.*, vol. 49, pp. 1573–1580, Sept. 2001.

[23] T. J. Licata, E. G. Colgan, J. M. E. Harper, and S. E. Luce, "Interconnect fabrication processes and the development of low-cost wiring for CMOS products," *IBM J. Res. Develop.*, vol. 39, no. 4, pp. 419–435, July 1995.

Francesco Bertazzi received the Laurea degree in electronics engineering from the Politecnico di Torino, Turin, Italy in 2000, and is currently working toward the Ph.D. degree in electronics engineering at the Politecnico di Torino.

His research is focused on the application of the FEM to waveguiding problems.

Giovanni Ghione (M'87–SM'94) received the Laurea degree in electronics engineering from the Politecnico di Torino, Turin, Italy, in 1981.

From 1983 to 1987, he was a Research Assistant with the Politecnico di Torino. From 1987 to 1990, he was an Associate Professor with the Politecnico di Milano, Milan, Italy. In 1990, he joined the University of Catania, Catania, Italy, as Full Professor of electronics. Since 1991, he has been a Full Professor with the II Faculty of Engineering, Dipartimento di Elettronica, Politecnico di Torino. Since 1981, he has been engaged in Italian and European research projects (ESPRIT 255, COSMIC, and MANPOWER) in the field of active and passive microwave CAD. His current research interests concern the physics-based simulation of active microwave and opto-electronic devices, with particular attention to noise modeling, thermal modeling, and active device optimization. His research interests also include several topics in computational electromagnetics, including coplanar component analysis. He has authored or coauthored over 150 papers and book chapters in the above fields.

Prof. Ghione is member of the Associazione Elettrotecnica Italiana (AEI). He is an Editorial Board member of the IEEE TRANSACTIONS ON MICROWAVE THEORY AND TECHNIQUES.

Michele Goano (M'98) received the Laurea and Ph.D. degrees in electronics engineering from the Politecnico di Torino, Turin, Italy, in 1989 and 1993, respectively.

In 1994 and 1995, he was a Post-Doctoral Fellow with the Département de Génie Physique, École Polytechnique de Montréal, Montréal, QC, Canada. In 1996, he joined the faculty of the Dipartimento di Elettronica, Politecnico di Torino. He was a Visiting Scholar with the School of Electrical and Computer Engineering, Georgia Institute of Technology, Atlanta, and with the Department of Electrical and Computer Engineering, Boston University, Boston, MA. He is currently involved in research on coplanar components, optical modulators, and wide-bandgap semiconductor devices.